La-induced changes in the magnetic and electronic properties of $Sr_{2-x}La_xFeMoO_6$

E. K. Hemery,[1,2] G. V. M. Williams,[1,2] and H. J. Trodahl[1]
[1]*MacDiarmid Institute for Advanced Materials and Nanotechnology, Victoria University, Wellington, New Zealand*
[2]*Industrial Research, P.O. Box 31310, Lower Hutt, New Zealand*

(Received 22 August 2005; revised manuscript received 15 May 2006; published 18 August 2006)

We report the results from a study of lanthanum doping in the Sr_2FeMoO_6 half-metallic double perovskites. The thermoelectric power systematically increases with electron doping, and the temperature dependence is remarkably similar to that reported in the superconducting cuprates. This suggests a common mechanism and we interpret the data in terms of a model applied to the superconducting cuprates. There is a systematic decrease in the saturation magnetization with La doping, which is predominately due to an increase in the Fe-Mo antisite disorder. Even though there is a large decrease in the saturation magnetization, surprisingly we find that the low-temperature magnetization can be described within the three-dimensional Heisenberg model. The saturation magnetization is shown to extrapolate to zero for ~44% antisite disorder, which is close to the maximum of 50% (i.e., completely random Mo-Fe site occupancy).

DOI: 10.1103/PhysRevB.74.054423 PACS number(s): 75.50.Bb, 72.15.Jf, 72.80.Ga, 75.47.−m

I. INTRODUCTION

The double perovskites have recently gained attention for their possible application in magnetoelectronic devices[1] due to their half-metallicity, large magnetoresistance, and high Curie temperature.[2] The most heavily studied in this class of material has been Sr_2FeMoO_6 (SFMO). Band structure calculations[2] are consistent with the Fermi level being within a band comprising an admixture of Mo(t_{2g}) and Fe(t_{2g}) orbitals and containing down-spin itinerant electrons, while the up-spin $Fe^{3+}3d^5$ electrons are localized within Fe(t_{2g}) and (e_g) orbitals.

Two main models have been proposed to account for the half-metallicity and the high Curie temperature in SFMO. The first model is based on double-exchange,[3–6] which is observed in the manganites. It has been argued that double-exchange occurs in SFMO, because the Curie temperature increases with increasing carrier concentration via partial substitution of Sr^{2+} by La^{3+}.[7] A similar increase in the Curie temperature was found in $Ca_{2-x}Nd_xFeMoO_6$, where Nd^{3+} is partially substituted onto the Ca^{2+} site.[8] However, Sarma *et al.*[9,10] argued that double-exchange does not occur in SFMO because the Fe $3d^5$ up-spin orbitals are full and hence, Hund's rule coupling cannot occur between the itinerant down-spin Mo $4d^1$ electron and the localized up-spin $3d^5$ electrons on the Fe site. Furthermore, the itinerant spins are in the opposite direction to the localized $3d^5$ electrons on the Fe site, which is again inconsistent with double-exchange. This leads to the second model of Fe $3d$ and Mo $4d$ hybridization and a strong exchange enhancement at the Mo site resulting in antiferromagnetic coupling between the localized Fe $3d^5$ up-spins and the itinerant Mo $4d^1$ down-spin.[9,10] It is assumed that there is significant hopping between Mo and Fe that leads to an admixture of down-spin Fe(t_{2g}) and Mo(t_{2g}) orbitals. The net result is that the Fermi level is contained within a band that has down-spin Fe(t_{2g}) and Mo(t_{2g}) character.

Strong Hund's rule coupling is expected to maintain Fe in a 3+ state consistent with $3d^5$ even in the presence of electronic doping, and it has also been suggested that there are holes in the oxygen $2p$ orbitals.[11] However, Mössbauer data have been interpreted in terms of a mixed Fe^{2+}/Fe^{3+} state in the pure compound.[12–14] A similar conclusion was reached from x-ray magnetic circular dichroism measurements.[15] Neutron diffraction measurements either show that there is no moment on the Mo site,[16] or a moment close to that expected for $S=1/2$ exists.[14] The appearance of a moment on the Mo close to that expected for Mo^{5+} appears to be inconsistent with the Fe $3d$-Mo $4d$ hybridization model mentioned above.

The effect of electronic doping on the magnetic and electronic properties is the key in furthering the understanding of SFMO. Previous studies have shown that electronic doping leads to an increase in the Curie temperature,[7,8] and photoemission spectroscopy data have been interpreted in terms of an increasing density of states at the Fermi level.[17] This has lead to the suggestion that the ferromagnetic state is mediated by the itinerant carriers via Ruderman-Kittel-Kasauya-Yosida (RKKY) coupling similar to that proposed to explain the ferromagnetic order in the dilute ferromagnetic semiconductors.[17] In the case of the dilute ferromagnetic semiconductors, it was shown that the Curie temperature increases with an increasing density of states at the Fermi level until a critical concentration beyond which the Curie temperature decreases.[18]

There is a clear need for further studies of electronic doping in SFMO. For this reason we have performed magnetic, transport, and structural measurements on $Sr_{2-x}La_xFeMoO_6$ and report the results in this paper.

II. EXPERIMENTAL DETAILS

Double perovskites were prepared by a solid-state reaction method from stoichiometric mixes of $Sr(NO_3)_2$, Fe_2O_3, MoO_3, and $La(NO_3)_2 \cdot 6H_2O$. The powder was denitrated at 700 °C in air. After pressing the powder at 40 000 kPa, the pellets were placed in air at 1200 °C for 4 h. The samples were then ground, pressed into pellets, and then sintered at 1100 °C in an atmosphere of 5% H_2–95% N_2 for 3 h. The latter process was repeated one more time, after regrinding

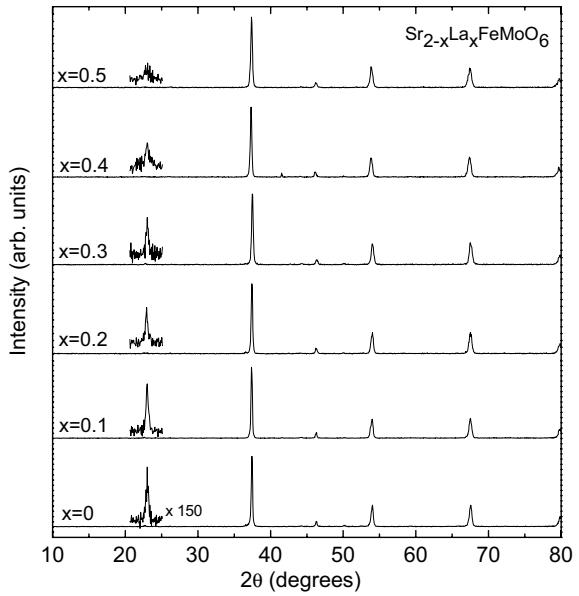

FIG. 1. XRD patterns of $Sr_{2-x}La_xFeMoO_6$ using Co Kα radiation. The insets show the expanded (101) peak that is also vertically offset.

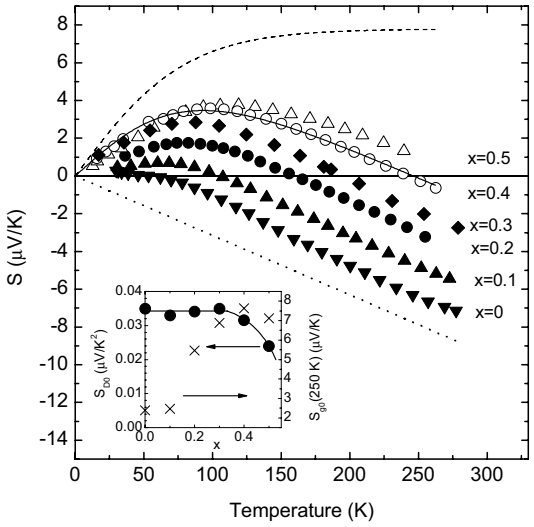

FIG. 2. Thermoelectric power versus temperature for $Sr_{2-x}La_xFeMoO_6$ samples with $x=0$ (filled down triangles), $x=0.1$ (filled up triangles), $x=0.2$ (filled circles), $x=0.3$ (filled diamonds), $x=0.4$ (open circles), and $x=0.5$ (open up triangles). The solid curve is a simulation of the $x=0.4$ data with a diffusion term (dotted curve) and a phonon-drag term (dashed curve). Inset: Plot of the diffusion thermoelectric power prefactor (filled circles, left axis) and the phonon drag thermoelectric power prefactor (crosses, right axis). The solid curve is a guide to the eye.

and repelleting, in order to remove any minority phase peak and obtain homogeneous samples. The phase composition and purity was determined from x-ray diffraction (XRD) measurements using Co Kα radiation. The electrical resistance were measured using the four-terminal method. The thermoelectric power was measured as a function of temperature using the standard temperature differential technique. It should be noted that unlike the resistivity, the thermoelectric power of these polycrystalline ceramics is not affected by high intergrain boundary resistance. It is affected by intergrain boundaries only if they develop a large thermal resistance, because the thermoelectric response is driven by the temperature gradient rather than by the electric field. Magnetization measurements to 700 K were made using a superconducting quantum interference devices (SQUID) magnetometer. A Quantum Design oven insert was used for measurements above 300 K.

III. RESULTS AND ANALYSIS

The room temperature XRD data from various $Sr_{2-x}La_xFeMoO_6$ samples are plotted in Fig. 1. They were normalized to the same (200) peak intensity. The XRD data shows single-phase material indexed to a tetragonal structure ($I4/mmm$ space group) with $a=5.59$ Å and $c=7.90$ Å. There is no evidence for a detectible change in the lattice parameters with La substitution. Evidently, the small reduction in the ionic radii with a maximal substitution of 25% La for Sr is not sufficient to change the lattice parameters by an amount that is detectible using our XRD setup.

It is important to know the degree of Fe-Mo antisite disorder (ASD) because it is thought to affect the saturation magnetization and Curie temperature as well as the magnetoresistance.[7,12,19,20] For this reason we measured the ASD fraction from the ratio, R, of the (101) peak intensity at 22.49° divided by the (200) peak intensity at 37.14°. Note that the (101) peak referenced to the double perovskites lattice is a superlattice spot in the underlying conventional perovskite lattice, and it must disappear for a full disordering of Fe and Mo. Sr_2FeMoO_6 is cubic above the Curie temperature, and the corresponding Miller index for the superlattice peak is (111). The (101) peak can be seen more clearly in the insets to Fig. 1, where it has been scaled by a factor of 150 and vertically offset. The relationship between R and the ASD was calibrated by modeling the XRD pattern using Powder Cell while the ASD was varied from 0 (complete order) to 50% (completely random Fe-Mo site occupancy). The following relationship was derived from these calculations, $R=0.001365(\mathrm{ASD})^2-0.136592(\mathrm{ASD})+3.417842$. The modeling assumes a random partition of the disorder, and this equation can also be used for similar double perovskite structures (e.g., Ba_2FeMoO_6 using a scaling factor of 1.72). The relationship was used to determine the ASD for the six samples, and we found values of 21.2, 22.6, 26.4, 25.9, 28.6, and 36.0% for $x=0$, 0.1, 0.2, 0.3, 0.4, and 0.5, respectively.

We find that there is a systematic increase in the thermoelectric power with increasing La concentration, as can be seen in Fig. 2. As mentioned above, the thermoelectric power is not affected by grain boundary resistance, and thus the data in Fig. 2 can be regarded as representing the thermoelectric power of the majority, intragrain material. The low-temperature peak and negative high temperature gradient for high La concentrations are similar to that reported by Fisher *et al.*[21] from thermoelectric power measurements on $Sr_{1.5}La_{0.5}FeMoO_6$.

The temperature dependence of the thermoelectric power is remarkably similar to that found in the superconducting

cuprates.[22] Furthermore, both classes of compounds show a systematic increase in the room temperature thermoelectric power with increasing electron doping. In the case of the superconducting cuprates, this correlation has proved to be a useful tool to estimate the doping state.[23] The close correspondence between the SFMO and superconducting cuprate thermopower suggests a common mechanism in both systems, even though the Fermi surfaces are different and the electronic state is three-dimensional (3D) for SFMO and two-dimensional (2D) for the superconducting cuprates.

In order to understand the thermoelectric power data one must note that the thermoelectric power has both a "diffusion" component S_d associated with only the electron gas and its dispersion, and a "phonon drag" component S_g arising from momentum delivered to the electrons when they scatter from phonons, and is thus related to the phonon dispersion and the electron-phonon interaction. In the simplest scenario these simply add so that the thermopower can be written as $S(T)=S_d(T)+S_g(T)$.

In the relaxation time approximation, the diffusion thermoelectric power in a cubic material can be written as[24]

$$S_d = -\frac{1}{eT\sigma}\int (\varepsilon-\mu)\left(-\frac{\partial f}{\partial \varepsilon}\right)\sigma(\varepsilon), \tag{1}$$

where

$$\sigma(\varepsilon) = (e^2/\Omega_0)\sum_k v(k)^2\tau(k)\delta[\varepsilon(k)-\varepsilon], \tag{2}$$

ε is the energy, μ is the chemical potential, f is the Fermi function, Ω_0 is the normalized volume, v is the quasiparticle velocity, and $\tau(k)$ is the scattering time. The dependence predicted by Eq. (1) is simply proportional to temperature if the density of states (DOS) is effectively constant within kT of the Fermi energy, but clearly very rapid changes in the DOS near the Fermi energy can lend more complex temperature dependencies to $S_d(T)$.

Although $S(T)$ could be modeled by assuming electron doping in the proximity to a sharp peak in the DOS,[25] that proposal would require structure within less than ~10 meV of the Fermi energy. This structure would need to remain that close even as the doping is changed by the introduction of as much as 0.5 La per formula unit, which appears to be highly unrealistic and not supported by band structure calculations.[11] In fact, band structure calculations show an increasing density of states for up to ~300 meV below and above the Fermi energy in the pure compound. Thus, assuming that the entire temperature dependence of $S(T)$ is due only to the proximity to a sharp peak in the DOS is untenable if it is to model the persistence of the systematic pattern over the large doping range in the present studies.

A more natural interpretation of $S(T)$ is available if phonon drag is included in the model, which has proved useful in interpreting the thermopower from the superconducting cuprates.[22] The drag component is expected to approximately mirror the phonon specific heat, rising at low temperature as phonons become thermally excited and saturating above the Debye temperature, Θ_D. In conventional metals the effect is attenuated at high temperatures where phonon-phonon scattering begins to dominate phonon-electron scattering, which then reduces the phonon-electron momentum exchange and leads to a $1/T$ dependence. On the assumption that phonon-electron scattering remains strong up to ambient temperature,[22] the phonon drag contribution is approximately proportional to the Debye function, rising from zero at zero temperature and saturating above Θ_D. Within this model the prediction is for a high-temperature thermoelectric power that consists of a constant phonon drag component and a diffusion component that is linear with temperature.[22] As the temperature is reduced the drag component falls and the total thermopower approaches zero at zero temperature, as required by the third law of thermodynamics. Within this model the high-temperature slope gives the diffusion term, and the extrapolation of that slope to zero temperature is the saturated drag component.[22]

Given the remarkable similarity between the thermopower in SFMO and the superconducting cuprates, we have also analyzed the thermopower data in terms of the same phonon drag model. In the present work we have chosen a phenomenological expression for the drag component and a temperature-linear diffusion component as $S(T)=S_{g0}\tanh(T/T_0)-S_{D0}T$. The resulting $S_g(T)$ (dashed curve), $S_d(T)$ (dotted curve), and $S(T)$ (solid curve) are plotted in Fig. 2 for x=0.4.

The values of S_{g0} (crosses) and S_{D0} (filled circles) are plotted in the inset to Fig. 2. It can be seen that S_{D0} is independent of x for x as high as 0.3 and decreases for higher La concentrations. This appears to suggest that doping effects on $S_d(T)$ are small for as much as 0.3 doped electrons per Mo if all the doped electrons appear in the down-spin conduction band with Fe(t_{2g}) and Mo(t_{2g}) character. We also find that S_{g0} increases for $x>0.2$ and appears to saturate for $x>0.4$. These results are understood by noting that the diffusion component depends primarily on the energy scale over which the DOS varies, evaluated at the Fermi energy. The small decrease in S_{D0} observed for $x=0.5$ is consistent with electron doping and an increasing Fermi energy based on band structure calculations and assuming a rigid band shift.[11] In contrast, the drag component is a very sensitive function of the balance between normal and umklapp scattering events, and that balance is strongly influenced by changes to the Fermi surface.[22,26]

The zero-field resistivity has been measured for all the samples and shows a small increase in the resistivity with decreasing temperature. There is an initial decrease in the magnitude of the resistivity and then a smaller decrease with increasing La concentration. The magnitude of the resistivity for the pure compound is comparable to that reported in other studies, but it is ~12 times greater than that reported from measurements on single crystals.[27] This suggests that the resistivity is dominated by the grain boundary resistance. The higher resistivity found in our pure sample may be due to a grain morphology that is different from that in the La-substituted samples.

It can be seen in Fig. 3 that there is a systematic decrease in the high-field magnetization with increasing La concentration. It has been suggested that this decrease is due to ASD as well as doping effects and that the saturation magnetiza-

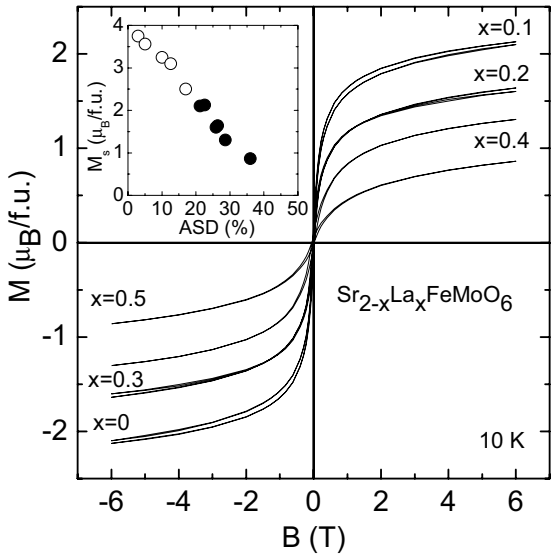

FIG. 3. Magnetization curves at 10 K for $Sr_{2-x}La_xFeMoO_6$. Inset: Plot of the magnetization at 6 T versus the ASD for this study (filled circles), and from Balcells *et al.*[12] for $x=0$ (open circles).

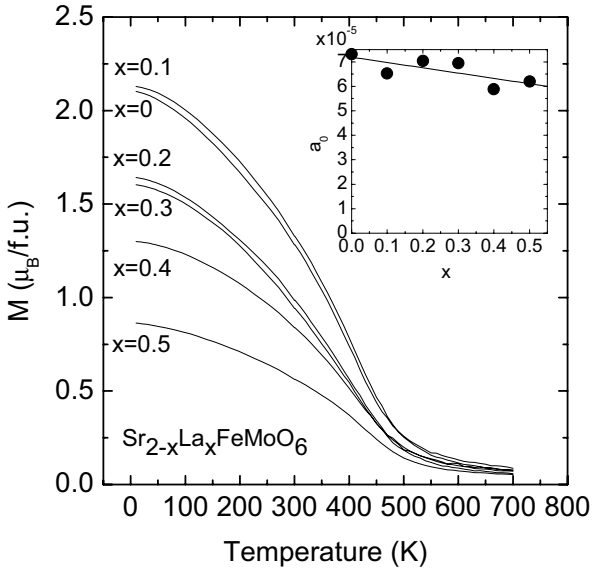

FIG. 4. Magnetization versus temperature at 6 T for $Sr_{2-x}La_xFeMoO_6$. Inset: Plot of prefactor for the low-temperature fit to the data as described in the text. The solid line is a linear best fit to the data.

tion can be written as $M_s=(1-2\times ASD)[m(\mathrm{Fe})-m(\mathrm{Mo})]+(1-2\times ASD)[\Delta m(\mathrm{Fe})-\Delta m(\mathrm{Mo})]$, where m(Fe) is the Fe moment, m(Mo) is the Mo moment, and Δm(Fe) and Δm(Mo) are the changes in the Fe and Mo moments by La doping.[7] This model assumes static moments on the Fe and Mo sites, as well as a Fe-Mo superexchange mechanism that leads to the magnetically ordered state. It also assumes that some of the electrons introduced by La doping appear on the Fe site. The situation is possibly more complicated, as we have mentioned earlier. For example, it has been suggested that Fe should remain in the 3+ state[11] and there is no well-defined Mo moment of 1 μ_B per formula unit, since for the pure compound the electron in the originally down-spin Mo(t_{2g}) orbital is itinerant.[10]

We find that the decrease in the high-field magnetization with increasing La doping can be primarily attributed to ASD, which is apparent in the Fig. 3 inset (filled circles). Also shown is data from the pure compound by Balcells *et al.*[12] (open circles). Our data is just a continuation of that found in the pure compound, and we find that $M_s=4.0-9\times ASD$. Consequently, by extrapolation we expect the magnetic order to disappear for ASD=44%, which is slightly less than the assumed 50%.[7]

Similar to a previous study,[7] we find that the Curie temperature, estimated from the maximum negative gradient of the magnetization data, increases with increasing La concentration. The magnetization at 6 T is plotted in Fig. 4, and we find that the Curie temperature, T_c, is 390±5 K, 390±5 K, 395±10 K, 395±10 K, 405±15 K, and 415±15 K for $x=0$, 0.1, 0.2, 0.3, 0.4, and 0.5, respectively. We have also fitted the low-temperature magnetization data to $M(T)=M_0(1-a_0T^n)$. We find that $n=1.5\pm0.1$ for all La concentrations, which is expected for a 3D Heisenberg ferromagnet. Surprisingly, we find that a_0 is only weakly dependent on La concentration, as can be seen in the inset to Fig. 4. Since a_0 is affected by the spin-wave dispersion, this result suggests that there is no significant change in the spin-wave dispersion for small wave vectors, even though there is a large change in M_0.

IV. CONCLUSIONS

In conclusion, the $Sr_{2-x}La_xFeMoO_6$ thermoelectric power displays a temperature dependence and shift with electron doping that is remarkably similar to that observed in the superconducting cuprates. We have modeled the La-induced changes in terms of electronic doping that affects the diffusion and the phonon-drag components. The decrease in the magnetization at 6 T with increasing La doping has been shown to be predominantly due to ASD. The high field magnetization is expected to be zero at ~44% ASD, which is slightly less than the 50% or completely random Fe-Mo site occupancy. Even in the presence of a large change in the ASD, we find that the low-temperature magnetization data can be interpreted within the 3D Heisenberg model, with only a small change in the spin-wave dispersion.

ACKNOWLEDGMENTS

We acknowledge funding support from the New Zealand Marsden Fund, the MacDiarmid Institute and the Royal Society of New Zealand. We thank L. Dupont for preparing and characterizing some of the samples.

[1] G. A. Prinz, Science **282**, 1660 (1998).
[2] K. -I. Kobayashi, T. Kimura, H. Sawada, K. Terakura, and Y. Tokura, Nature (London) **395**, 677 (1998).
[3] J. S. Kang, H. Han, B. W. Lee, C. G. Olson, S. W. Han, K. H. Kim, J. I. Jeong, J. H. Park, and B. I. Min, Phys. Rev. B **64**, 024429 (2001).
[4] T. Saitoh, M. Nakatake, A. Kakizaki, H. Nakajima, O. Morimoto, Sh. Xu, Y. Moritomo, N. Hamada, and Y. Aiura, Phys. Rev. B **66**, 035112 (2002).
[5] B. Martínez, J. Navarro, L. I. Balcells, and J. Fontcuberta, J. Phys. Condens. Matter **12**, 10515 (2000).
[6] Y. Moritomo, Sh. Xu, A. Machida, T. Akimoto, E. Nishibori, M. Takata, and M. Sakata, Phys. Rev. B **61**, R7827 (2000).
[7] J. Navarro, C. Frontera, L. Balcells, B. Martinez, and J. Fontcuberta, Phys. Rev. B **64**, 092411 (2001).
[8] D. Rubi, C. Frontera, J. Fontcuberta, M. Wojcik, E. Jedryka, and C. Ritter, Phys. Rev. B **70**, 094405 (2004).
[9] D. D. Sarma, P. Mahadevan, T. Saha-Dasgupta, S. Ray, and A. Kumar, Phys. Rev. Lett. **85**, 2549 (2000).
[10] D. D. Sarma, Curr. Opin. Solid State Mater. Phys. **5**, 261 (2001).
[11] T. Saitoh, M. Nakatake, H. Nakajima, O. Morimoto, A. Kakizaki, S. Xu, Y. Moritomo, N. Hamada, and Y. Aiura, Phys. Rev. B **72**, 045107 (2005).
[12] L. I. Balcells, J. Navarro, M. Bibes, A. Roig, B. Martinez, and J. Frontcuberta, Appl. Phys. Lett. **78**, 781 (2001).
[13] J. Lindén, T. Yamamoto, M. Karppinen, H. Yamauchi, and T. Pietari, Appl. Phys. Lett. **76**, 2925 (2000).
[14] O. Chmaissem, R. Kruk, B. Dabrowski, D. E. Brown, X. Xiong, S. Kolesnik, J. D. Jorgensen, and C. W. Kimball, Phys. Rev. B **62**, 14197 (2000).
[15] M. Besse, V. Cros, A. Barthélémy, H. Jaffrès, J. Vogel, F. Petroff, A. Mirone, A. Tagliaferri, P. Bencok, P. Decorse, P. Berthet, Z. Szotek, W. M. Temmerman, S. S. Dhesi, N. B. Brookes, A. Rogalev, and A. Fert, Europhys. Lett. **60**, 608 (2002).
[16] B. García-Landa, C. Rittter, M. R. Ibarra, J. Blasco, P. A. Algarabel, R. Mahendiran, and J. García, Solid State Commun. **110**, 435 (1999).
[17] J. Navarro, J. Fontcuberta, M. Izquierdo, J. Avila, and M. C. Asensio, Phys. Rev. B **69**, 115101 (2004).
[18] T. Dietl, H. Ohno, and F. Matsukura, Phys. Rev. B **63**, 195205 (2001).
[19] A. S. Ogale, S. B. Ogale, R. Ramesh, and T. Venkatesen, Appl. Phys. Lett. **75**, 537 (1999).
[20] J. Navarro, L. I. Balcells, F. Sandiumenge, M. Bibes, A. Roig, B. Martínez, and J. Fontcuberta, J. Phys. Condens. Matter **13**, 8481 (2001).
[21] B. Fisher, K. B. Chashka, L. Patlagan, and G. M. Reisner, Curr. Appl. Phys. **4**, 518 (2004).
[22] H. J. Trodahl, Phys. Rev. B **51**, R6175 (1995).
[23] S. D. Obertelli, J. R. Cooper, and J. L. Tallon, Phys. Rev. B **46**, R14928 (1992).
[24] R. D. Barnard, *Thermoelectricity in Metals and Alloys* (Taylor and Francis, London, 1972).
[25] G. C. McIntosh and A. B. Kaiser, Phys. Rev. B **54**, 12569 (1996).
[26] V. A. Rowe and P. A. Schroeder, J. Phys. Chem. Solids **31**, 1 (1970).
[27] Y. Tomioka, T. Okuda, Y. Okimoto, R. Kumai, K.-I. Kobayashi, and Y. Tokura, Phys. Rev. B **61**, 422 (2000).